СООБЩЕНИЯ
ОБЪЕДИНЕННОГО
ИНСТИТУТА
ЯДЕРНЫХ
ИССЛЕДОВАНИЙ
ДУБНА

E1 - 11542

M.Klein, W.-D.Nowak

EXTRAPOLATION OF DEEP INELASTIC LEPTON-NUCLEON CROSS SECTIONS TO SPS ENERGIES

1978

E1 - 11542

M.Klein, W.-D.Nowak

EXTRAPOLATION OF DEEP INELASTIC LEPTON-NUCLEON CROSS SECTIONS TO SPS ENERGIES

Кляйн М., Новак В.-Д. **E1 - 11542**

Экстраполяция сечений глубоконеупругого рассеяния в области энергий СПС

Данные по двойному дифференциальному сечению глубоконеупругого рассеяния лептонов экстраполируются из изученной к настоящему моменту кинематической области в область, где будут получены данные о совместном Дубна-ЦЕРН-Мюнхен-Сакле мюонном эксперименте. Обсуждаются относительные погрешности процедуры такой экстраполяции и показано, что они не превышают фактора 2.

Работа выполнена в Лаборатории высоких энергий ОИЯИ.

Сообщение Объединенного института ядерных исследований. Дубна 1978

Klein M., Nowak W.-D. **E1 - 11542**

Extrapolation of Deep Inelastic Lepton-Nucleon Cross Sections to SPS Energies

Double differential deep-inelastic lepton scattering cross sections and counting rates are extrapolated from existing data to kinematical regions which will be explored in the Dubna-CERN-Munich-Saclay muon experiments. Uncertainties of this extrapolation procedure are discussed and found to be limited by a factor of about two.

The investigation has been performed at the Laboratory of High Energies, JINR.

Communicotion of the Joint Institute for Nucleor Research. Dubno 1978

1. INTRODUCTION

One of the large spectrometers currently constructed at the CERN SPS, called NA4, is designed to measure inclusive deep inelastic muon scattering in an entirely new kinematic region [1]. Exposing different targets to a high intensity muon beam of about 280 *GeV* maximum energy, four-momentum transfers q^2 of hundreds of $(GeV/c)^2$ are reached which will probe the nucleon structure at a new level. During the physical preparation and the analysis of the NA4 experiments it is required to estimate the double differential lepton-nucleon cross section $d\sigma/da\,db$, and counting rates, respectively. Thus we have written a program, FRAME, to calculate $d\sigma$ on the basis of available experimental results.

The extrapolation of the cross section to the new kinematic region is influenced by scaling violations and other uncertainties which are discussed in Sec. 2. Due to statistics the NA4 kinematic range effectively decreases to an extent depending on the beam intensity, target material and length. Some typical examples are given in Sec. 3. Section 4 contains the user's guide for FRAME. A brief summary is given in Sec. 5.

2. UNCERTAINTIES OF EXTRAPOLATIONS TO THE NEW KINEMATIC REGION

Exact scaling would allow one to predict $d\sigma/dq^2d\nu$ (*fig. 1* and *tabl. 1*) already from the first MIT SLAC experiments [2] covering a very restricted (q^2,ν) region. La-

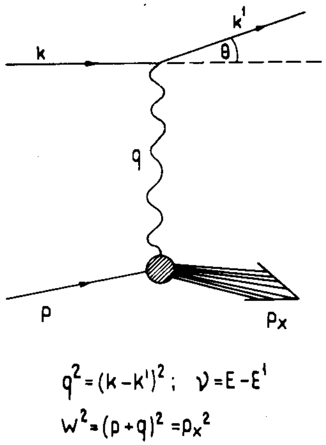

Fig. 1 ---

ter experiments, however, discovered scaling violations[3-6] which make the extrapolation of low q^2 measurements to some extent uncertain. In order to estimate this uncertainty we study the pattern of scaling violations.

Scale breaking effects have been found to be consistent with asymptotically free gauge theories[7]. Considering the moments of structure functions, the canonical scaling behaviour is modified by some powers of $\log(q^2)$, e.g.,

$$\int_0^1 dx\, x^{n-2}\, \nu W_2(x,q^2) \xrightarrow[q^2\to\infty]{} a(n)\cdot(\log(q^2/\mu^2))^{b(n)} \qquad (1)$$

with some functions $a(n), b(n)$ and mass scale μ^2. For our purposes, this specific behaviour suggests to plot the kinematic regions covered experimentally as functions of $\log(q^2)$ and x (*fig. 2*). The following abbreviations are used: S75: SLAC experiment studying the turn-on of scaling[8]; S69,74: SLAC electroproduction[2,3]; F76: Fermilab 147 *GeV* μD[4] and the μFe scaling test experiment[5]; F77: Fermilab 147 *GeV* μp[6]. In the logarithmic scale the extension of the q^2 range by NA4 appears to be lessened. Thus the presently discovered pattern of scaling violations will not be responsible for

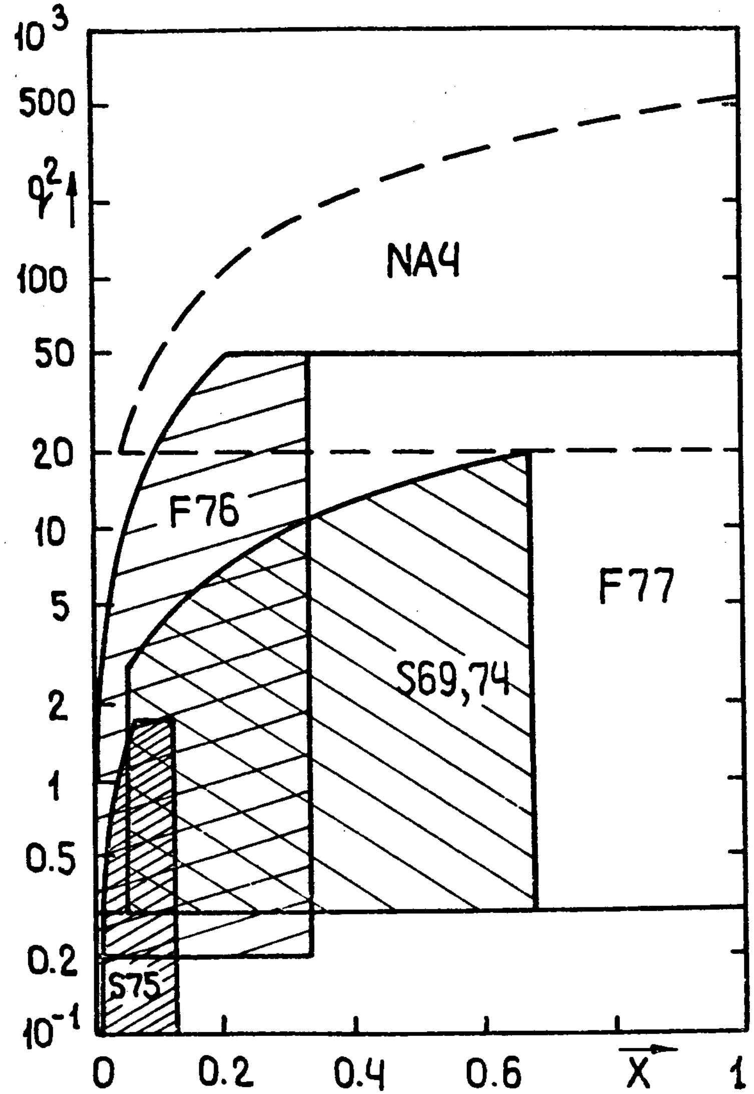

Fig. 2. $(\log q^2, x)$ *regions covered by deep inelastic experiments.*

an important uncertainty of the extrapolated cross sections *.

Uncertainties arise also because in practice fits for νW_2 are used which, at best, are valid in the region shown in *fig. 2*. The resulting superposition of both effects might be deduced from *fig. 3* where different parametrizations of νW_2 (Sec. 4, eqs. 4-7) are plotted as functions of x at a typical large value of q^2 for NA4. With the exception of very small x the uncertainty will not exceed a factor of about two. For $x < 0.7$ differences arise dominantly from the different scaling behaviour (compare F76, F77, e.g., with the scale invariant quark parton model fit (BP)/9/). In the region above $x \sim 0.7$ νW_2 is very small and it becomes difficult to decide whether scaling violations or features of the fit are responsible for the main uncertainty of the extrapolation.

Additional uncertainties arise from an inperfect determination of the other structure function W_1, i.e., the ratio $R(q^2, \nu) = \sigma_\ell / \sigma_t$ (*tab. 1*). The data agree with a rather small R $(0 \leq R \leq 0.5)$ being only weakly dependent on q^2 and ν. If R is assumed to be constant a mean value $\bar{R}$ of about 0.2 is favoured which seems to be independent of the target material /3/. The uncertainty arising from changes of R can be visualized plotting the ratio

$$\frac{d\sigma(q^2, \nu; R)}{d\sigma(q^2, \nu; \bar{R})} = \frac{y^2/(1+R) + 2(1-y)}{y^2/(1+\bar{R}) + 2(1-y)} . \qquad (2)$$

This ratio is a function of $y = \nu/E$ and R only. It can be seen from *fig. 4* that the uncertainty increases for $y \to 1$,

---

* There are new data available from two Fermilab muon experiments reaching a maximum q^2 of 150 $(GeV/c)^2$ and being consistent with the elder results on scaling violations /11/.

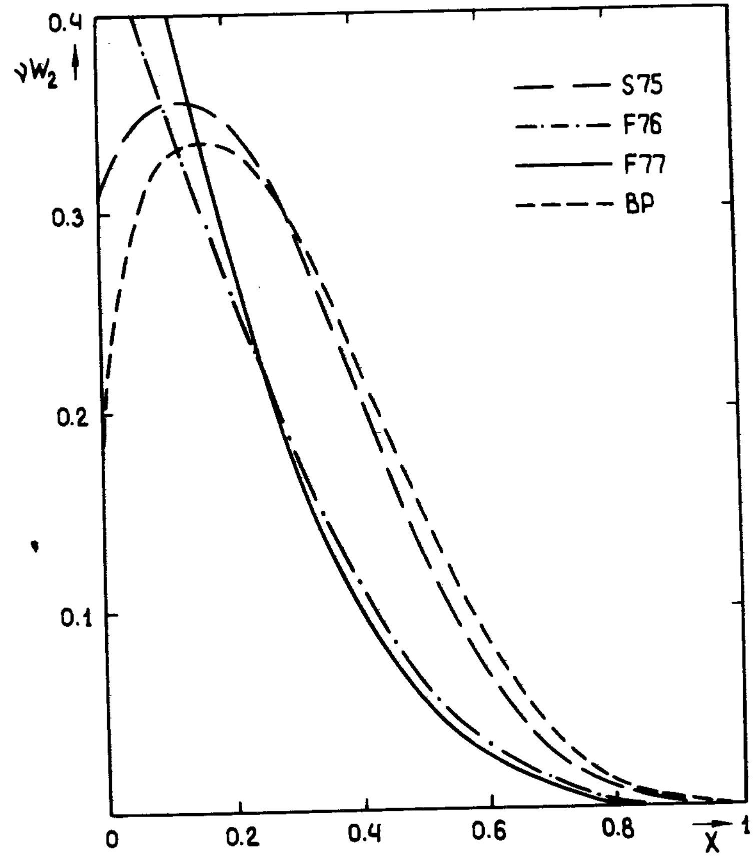

Fig. 3. Different fits of νW_2 *vs.* x *at* $q^2 = 200 (GeV/c)^2$.

but is limited to ~20%. This expresses the well-known fact that the measurement of R requires to explore the high y region where the cross section is sensitive to changes of R.

3. THE INFLUENCE OF COUNTING RATES ON THE EXTENSION OF RANGE

Counting rates expected can be calculated if the beam intensity is known as a function of energy (for intensities

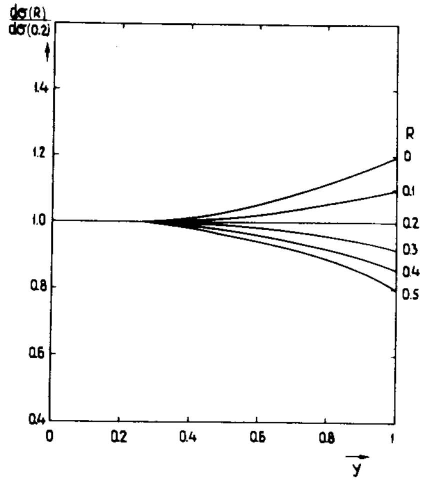

Fig. 4. Ratio $d\sigma(R)/d\sigma(\bar{R})$ *vs.* $y=\nu/E$ *for* $\bar{R}=0.2$ *(eq.2).*

see [1]). Far from discussing the whole problem of rates for NA4 experiments, we give some typical examples in order to visualize the influence of rates on $d\sigma$, in particular on the maximum q^2 reachable.

Figures 5 and *6* show (q^2,ν) curves for counting rates per day at $E = 280$ *GeV* for 50 *m* carbon and hydrogen targets, respectively. A 20x20 binning in (x,y) has been applied which corresponds to the expected experimental resolution of a few per cent[1]*. The carbon target option as the most effective one (*fig. 5*) allows to reach a region of x up to ~ 0.8 and a q^2 maximum of about 400 *(GeV/c)*^{2} within a 10% statistical accuracy (for 10 days running time). One should note that in the large q^2 region the equirate lines are weakly dependent on ν. As a consequence, a restriction of $y=\nu/E$ to 0.8-0.9 does not affect remarkably the maximum of q^2 practically reachable. We have also included in *fig. 6*, for hydrogen, the corresponding equirate lines at lower

---

* We have tested that the resulting curves are almost independent of the chosen binning, whether (x,y) or (q^2,ν), and of the numbers of bins as long as these are around 15.

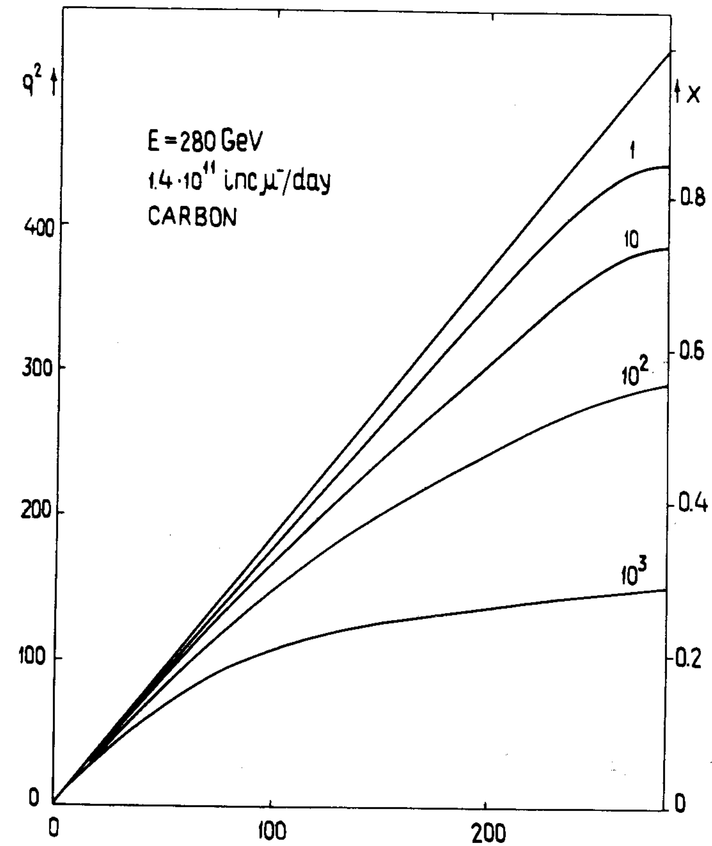

Fig. 5. Events rates per day expected for NA4 using a 50 m carbon target at $E = 280$ *GeV.*

energy (dashed curves for $E = 200$ *GeV*). It becomes apparent that the main advantage of increasing the energy from 200 to 280 *GeV* is an extension of the ν range only, at least with respect to the counting rates. Due to the beam spectrum, the maximum q^2 reached at a reasonable statistical accuracy is larger at the lower than at the higher energy.

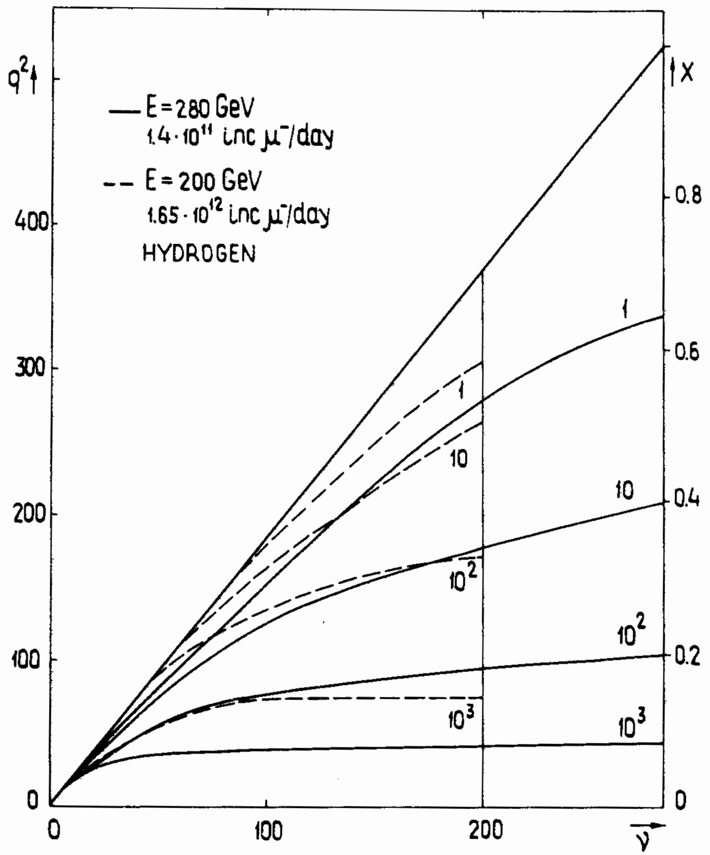

Fig. 6. Event rates per day expected for NA4 using a 50 m hydrogen target at E = 280 GeV (solid curves) and at E = 200 GeV (dashed curves).

4. *USER'S GUIDE TO FRAME*

FRAME allows to calculate $d\sigma/da\,db$ or rates simultaneously for 6 different sets of (a,b), namely (q^2,ν), (q^2,W), (q^2,W^2) (E',θ), (x,y) and (q^2,x), and altogether for 9 different modes to plot the results, e.g., the (q^2,ν) plot in bins of (x,y). In *tab. 1* all coded formulae are listed the choice of which is controlled by the

Table 1

Compilation of Formulae Coded in FRAME

IPAR	Cross section	Plotted in equidistant bins of	Boundaries
1	$d\sigma/dq^2d\nu = \Sigma = (2\pi\alpha^2 \cdot \nu W_2/q^4E^2)$ $\times [\frac{q^2}{2\nu}\,\frac{1-R}{1+R} + \frac{\nu}{1+R} + \frac{2E}{\nu}(E-\nu)]$	q^2,ν	$q^2_{max} = s = 2ME$ $\nu_{max} = E$, $q^2 \leq 2M\nu$
2	$d\sigma/dq^2dW = \frac{W}{M}\cdot\Sigma$	q^2, W	$M \leq W \leq (M^2+s)^{1/2}$ $q^2 \leq M^2+s-W^2$ $(y \leq 1)$
3	$d\sigma/dq^2dW^2 = \frac{1}{2M}\cdot\Sigma$	q^2, W^2	$M^2 \leq W^2 \leq (M^2+s)$ $q^2 \leq M^2+s-W^2$ $(y \leq 1)$
4	$d\sigma/dE'd\Omega = (\frac{d\sigma}{d\Omega})_{Mott}\frac{1}{E-E'}\cdot\nu W_2$ $\times\{1+\frac{1}{1+R}(2\tan^2\frac{\theta}{2}+\frac{(E-E')^2}{2EE'\cos^2\frac{\theta}{2}}\}$ $(d\sigma/d\Omega)_{Mott} = \frac{\alpha^2\cos^2\frac{\theta}{2}}{4E^2\sin^4\frac{\theta}{2}}$	E', θ	$E'_{min} \leq E' \leq E$ where E'_{min} sets an (arbitrary) upper limit for θ. up to now E'_{min} determined by $y_{max} = 0.95$ chosen in FRAME. $\sin^2\frac{\theta}{2} \leq \frac{M}{2}(\frac{1}{E'}, -\frac{1}{E})$
5	$\frac{d\sigma}{\Gamma_t\,dE'd\Omega} = \sigma_t + \epsilon\sigma_\ell = \frac{E(E-\nu)}{\pi\Gamma_t}\cdot\Sigma$ $\epsilon = 1/(1+\frac{2(q^2+\nu^2)}{4EE'-q^2})$	x, ϵ ϵ corresp. to $y = 1-\frac{1}{\epsilon}+\sqrt{\frac{1}{\epsilon^2}-1}$	$0 \leq x, \epsilon \leq 1$
6	$d\sigma/dx\,dy = \frac{2\pi\alpha^2}{s(xy)^2}(\frac{y^2}{1+R} + 2(1-y))\cdot\nu W_2$	x, y	$0 \leq x, y \leq 1$
7	$d\sigma/dq^2d\nu$	x, y	see IPAR = 1
8	$d\sigma/dq^2dW^2$	x, y	see IPAR = 3
9	$d\sigma/dq^2dx = \frac{\nu}{x}\cdot\Sigma$	q^2, x	$q^2 \leq sx$

parameter IPAR. The fourth column of *tab. 1* gives the kinematic limits of the variables used.

The structure function W_1 is expressed by W_2 according to

$$W_1 = W_2 (1 + \nu^2/q^2)/(1 + R), \tag{3}$$

where R is assumed to be independent of q^2 and ν as discussed above. We used the following three parametrizations for νW_2 according to the experiments mentioned.

i) S75 /8/

$$\nu W_2 = (1 - W_2^{el}(q^2)) \sum_{n=3}^{7} a_n (1-x')^n , \tag{4}$$

where W_2^{el} is a small correction to $1 (\sim 1/q^4)$ related to the proton form factors ("closure approximation"), and $a_3 = 1.0621$, $a_4 = -2.2594$, $a_5 = 10.54$, $a_6 = -15.8277$, $a_7 = 6.7931$;

ii) F76 /4/

$$\nu W_2 = (1 + a \cdot \ln q^2/3 \; \ln 1/6x) \sum_{n=3}^{5} b_n (1-x)^n \tag{5}$$

with

$a = 0.072$, $b_3 = 0.746$, $b_4 = 0.540$, $b_5 = -0.997$, q^2 in $(GeV/c)^2$;

iii) F77 /6/

$$\nu W_2 = \exp(a \ln q^2/3 \; \ln 1/6x) \sum_{n=3}^{5} c_n (1-x)^n \tag{6}$$

with

$a = 0.145$, $c_3 = 2.799$, $c_4 = -4.048$, $c_5 = 1.615$, q^2 in $(GeV/c)^2$.

Note that a scale breaking parametrization as in eqs. 5,6 leads to parameters a which seem to depend on the target used, i.e., $a = 0.072 \pm 0.038$ for D (eq. 5), $a = 0.145 \pm 0.024$ for H_2 (eq. 6), and $a = 0.099 \pm 0.018$ for Fe /5/. In estimating $d\sigma$, formula (6) can be preferred because the experiment /6/ has the largest overlapping with NA4 (see *fig. 2*).

Table 2

Data cards of FRAME

FELD	IW2	NCA	NCB	JSN
ENER	$(E, XNP)_1$, $(E, XNP)_2$, ... up to 16 beam energies E in *GeV* and corresponding beam intensities XNP			
PARA	IPAR			
ROIN	RHO	R		

IW2	denotes the parametrization of νW_2 used i.e., IW2=1 (eq. 4); IW2=2 (eq. 5); IW2=3 (eq. 6); IW2 4 (eq. 7); IW5=5 all parametrizations.
NCA NCB	number of bins
JSN	JSN=1 cross sections; JSN=2 counting rates
XNP	number of incident particles per day, for convenience to divide by 10^{10}
RHO	target thickness times length in *g/cm*^{2}
R	σ_ℓ / σ_t (see Sec. 2).

iv) BP /9/

As a first choice for a scale invariant νW_2 we included a formula obtained by Barger and Phillips in a valence quark parton model.

$$\nu W_2 = x^{1/2} [0.272(1-x^2)^3 + 0.228(1-x^2)^5 + 0.345(1-x^2)^7] + 0.193(1-x)^9 . \tag{7}$$

Using FFREAD /10/ the program reads 4 data cards free of ordering and format which are listed and explained in *tab. 2*. According to the chosen block structure of FRAME one can easily add other expressions for νW_2 (to be inserted into FUNCTION W2NU) or/and $d\sigma$ (to be inserted into FUNCTION D2SIG).

5. SUMMARY

Using available deep inelastic data we have discussed the expected double differential cross sections for the muon experiment NA4. We have written and used a corresponding program which calculates $d\sigma/da\,db$ for many sets of (a,b) and modes to plot the results. Uncertainties were discussed of extrapolating previous results to the new kinematic region and were found to be limited by a factor of about two. Examples for carbon and hydrogen targets were given to visualize the influence of counting rates on the extension of the kinematic range.

REFERENCES

1. *Proposal and Addenda of the NA4 experiment CERN/SPSC/74-79,-103,-108,-120 and 77-12/P19.*
2. *Bloom E. et al. Phys.Rev.Lett., 1969, 23, p.930; Breidenbach M. et al. Phys.Rev.Lett., 1969, 23, p.935.*
3. *Poucher J. et al. Phys. Rev.Lett., 1974, 32, p.118.*
4. *Anderson H. et al. Phys.Rev.Lett., 1976, 37, p.4.*
5. *Watanabe Y. et al. Phys.Rev.Lett., 1975, 35, p.898. Chang C. et al. Phys.Rev.Lett., 1975, 35, p.901.*
6. *Anderson H. et al. Phys.Rev.Lett., 1977, 38, p.1450.*
7. *Politzer H. Phys.Rev., 1974, 14C, no. 4. Tung W.-K. Phys.Rev., 1975, D12, p.3613. Hinchliffe I., Llewellyn-Smith C.H. Nucl.Phys., 1977, B128, p.93.*
8. *Stein S. et al. Phys.Rev., 1975, D12, p.1884.*
9. *Barger V., Phillips R. Nucl.Phys., 1974, B73, p.269.*
10. *Brun R. et al. FFREAD User's Guide, CERN DD 77/11, 1977.*
11. *Hand L. Inv. Talk at the Lepton-Photon Symposium, Hamburg, 1977.*

Received by Publishing Department on May 4 1978.